Experimental and CFD Analyses Examining Ozone Distribution in a Model Room with a Two-dimensional Flow Field

K Ito[1], S Kato[2], DN Sørensen[3], and CJ Weschler[3]

[1]Tokyo Polytechnic University, Kanagawa, Japan
Email: ito@arch.t-kougei.ac.jp   http://www.arch.t-kougei.ac.jp/ito
[2]IIS, University of Tokyo, Tokyo, Japan
[3]ICIEE, Technical University of Denmark, Lyngby, Denmark

Summary: *This paper reports the results of room model experiments and Computational Fluid Dynamics (CFD) analysis of ozone distribution in indoor air. The analyzed room model had one supply inlet and one exhaust outlet, with a cavity of dimensions 1.5m (x) × 0.3m (y) × 1.0m (z) in which a two-dimensional flow field was developed. In order to discuss the order of wall surface deposition for ozone, the concentration distributions of ozone in the model room were measured. CFD analysis corresponding to the experimental conditions and with a built-in ozone wall surface deposition model was carried out. The results of CFD prediction were in good agreement with the room model experiment.*

Keywords: Computational Fluid Dynamics, Surface deposition, Ozone, Room model experiment
Category: Modelling Technique

1 Introduction

Recently, it has been confirmed that ozone in room air actively generates various free radicals by reacting with the organic and inorganic compounds existing in the air [Weschler, 2000]. The free radicals and other products of chemical reactions are often more irritating than their precursors. In particular, the products of ozone/terpenes reactions cause greater airway irritation in mice than would be predicted based on the known response of mice to ozone or terpenes [Wolkoff et al., 1999]. Such chemical reactions can significantly alter the concentrations of indoor pollutants [Nazaroff et al., 1986; Weschler, 2000]. Furthermore, heterogeneous reactions between ozone and various surfaces occur, which further reduce the ozone concentration and must be considered in the ozone balance of indoor environments.

Weschler and Shields (2000) have simulated chemical reactions in indoor air using mass balance models and assuming perfect mixing; these simulations examined the influence of ventilation rates on uni- and bimolecular reactions. Using computational fluid dynamic (CFD) simulations, Sørensen and Weschler (2002) have reported the distribution of chemical compounds resulting from various indoor chemical reactions. However, there is insufficient data to experimentally verify the two-dimensional or three-dimensional distributions resulting from chemical reactions in indoor air.

Here, we isolate the surface reactions and measure the distribution of ozone within a 2D model room. The results are used to validate a CFD model, corresponding to the experimental set-up, including surface deposition of ozone.

2 Equation for Ozone Transportation

Assuming the concentration of ozone at a point in space to be C_o [ppm], the transportation of ozone is expressed by Equation (1):

$$\frac{\partial \overline{C_o}}{\partial t} + \frac{\partial \overline{U_j}\,\overline{C_o}}{\partial x_j} = \frac{\partial}{\partial x_j}\left(\left(D_o + \frac{\nu_t}{\sigma_t}\right)\cdot\frac{\partial \overline{C_o}}{\partial x_j}\right) \quad (1)$$

Here, Overbar ($^{-}$) denotes the ensemble-mean value. D_o [m²/sec] is the molecular diffusion coefficient of ozone in the gas phase, $\overline{U_j}$ [m/sec] is the ensemble-mean velocity, ν_t [m²/sec] is the turbulent eddy viscosity, and σ_t [-] is the turbulent Schmidt number.

3 Modeling the Wall Surface Deposition Flux of Ozone

The surface deposition of the local concentration close to the surface and, from molecular theory, the flux at the surface is given by (Cano-Ruiz et al., 1993):

$$Js = -\gamma \frac{\langle v \rangle}{4} C_o \big|_{y=\frac{2}{3}\lambda} \quad (2)$$

Here, γ [-] is the mass accommodation coefficient; $<v>$ [m/s] is the Boltzmann velocity for ozone; λ [m] is the mean molecular free path (6.5×10^{-8}). However, the grid scale (on the order of 10^{-8} [m]) is very small compared to the length scales necessary to resolve the flow field and concentration field within the CFD model. In this paper, to enable an increased length scale at the surface, the following flux model is adopted [Sørensen and Weschler, 2002]:

$$Js = -\frac{\gamma \cdot \dfrac{\langle v \rangle}{4}}{1 + \gamma \cdot \dfrac{\langle v \rangle}{4}\cdot \dfrac{\Delta y_1}{D_o}} \cdot C_o \big|_{y=\Delta y_1} \quad (3)$$

Here, Δy_1 is the distance to the center of the first computational cell ($\Delta y_1 < y^+=1$). The value used for the mass accommodation coefficient, γ, to stainless steel was 8.0×10^{-6} (Cano-Ruiz et al., 1993).

4 Outline of Model Room Experiment

Experiments were conducted in a model room to measure quantitatively the concentration of ozone at different locations in the indoor air. The perspective layout of the model room and a photo of its external appearance are shown in Figure 1. The model is a cavity measuring 1.5 [m] (x) × 0.3 [m] (y) × 1.0 [m] (z) in which a two-dimensional mean flow field is developed. It is equipped with 0.02 [m] wide inlet and outlet slots. The supply inlet slot is positioned along the ceiling, and the exhaust outlet slot is set along the ceiling on the other sidewall. The four boundaries – ceiling, floor, right, and left walls – were made of SUS 304 stainless steel and the others were glass. The deposition of ozone onto glass is known to be comparatively small [Cano-Ruiz et al., 1993] and is neglected.

The air inlet velocity (U_{in}) was set at 3.0 [m/s] (air change rate: 144 [times/h]) and 2.0 [m/s] (96 [times/h]). The inlet air and all the walls were maintained at isothermal conditions (293 ± 1.0 [K]). The supply air was passed through activated carbon and HEPA filters to keep the concentration of background contaminants low. In order to prevent photochemical reaction of ozone, the model room experiments were carried out in a dark room. The central section in the Y direction is taken as the measurement plane (x-z plane). Points of measurement in the model room are shown in Figure 2.

5 Measurement Data and Method

In this experiment, the target chemical compound was ozone. Ozone was assumed to have entered the supply airflow by infiltration from the outdoor air. Two levels of C_{in} were considered at concentrations of 0.65 and 2.44 [ppm], respectively. The ozone concentrations used in these experiments were relatively high compared with typical outdoor concentrations. Ozone was analyzed using a UV Photometric Analyzer at a wavelength of 254 [nm]; its concentration range was 0 - 9.999 [ppm], and its precision was 0.001 [ppm]. GC/MS was used for the background volatile organic compounds (VOC). The sampling flow rate of the UV Photometric Analyzer was 1.5 [L/min] and the ozone concentration was calculated as a time-averaged concentration over ten minutes. The experimental cases are shown in Table 1.

6 Outline of Numerical Analysis

The flow fields and diffusion fields for ozone were analyzed, targeting the room model. An outline of the space analyzed is given in Figures 1 and 3. When the air supply slot width is the representative length (L_0=0.02 [m]), the analytical space is a two-dimensional room measuring $75L_0$ (x) × $50L_0$ (z) (=1.5 [m] × 1.0 [m]). Flow fields were analyzed
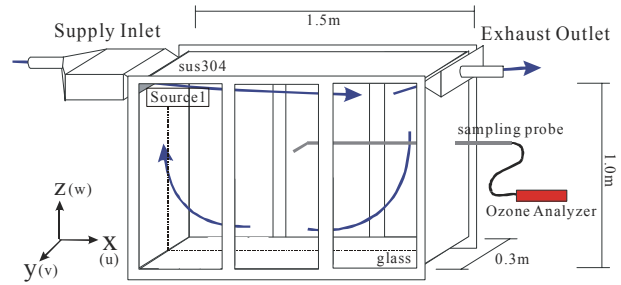
(a) Perspective layout of model room

(b) Photo of external appearance
Figure 1 Model room (experiment)

Table 1 Experimental case

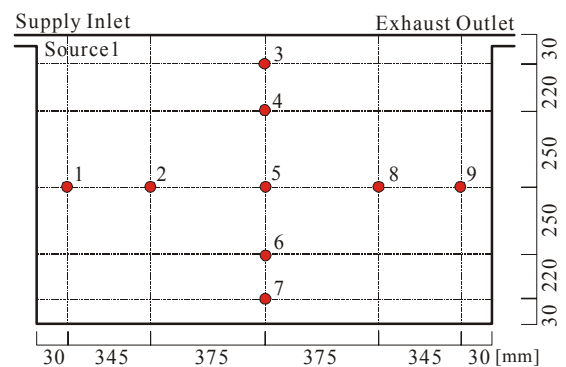| Exp. Case	C_{in} [Ozone]	Supply Velocity [U_{in}]
Case (e1-a)	0.65 ppm	3.0 m/s
Case (e1-b)		2.0 m/s
Case (e2-a)	2.44 ppm	3.0 m/s
Case (e2-b)		2.0 m/s

Figure 2 Measurement points in model room

using the low Reynolds number type k-ε model [Murakami et al., 1996]. The QUICK scheme is used for the convection term, and the SIMPLE algorithm is used. To analyze the flow field in the boundary layer, the center of the computational cells closest to the wall surface should be at a non-dimensional distance (Wall Unit) of $y^+<1$, where $y+ = u*y_1/\nu$, where y_1 is the distance normal to the wall surface, ν is the kinematic viscosity, and $u* = \sqrt{\tau_w/\rho}$ is the frictional velocity.

Here, ρ is the air density and τ_w is the wall shear stress. The concentrations of ozone were analyzed with the wall surface deposition flux model shown in Equation (3). An unequal interval mesh is used for this analysis; the height of the cells closest to the ceiling wall surface is 0.006 [mm], which ensured that, for the grid points at the walls, y+ was <1 everywhere inside the room. Numerical conditions are given in Table 2.

7 Numerical Cases

This analysis focused on the heterogeneous reactions of ozone, which are assumed to occur at the wall surfaces in the model room. The generation rate of ozone from the supply inlet (Source 1 in Figure 1) mirrored the conditions in the experiment. The room temperature was assumed to be a constant at 293 [K].

The numerical cases are shown in Table 3. In Case (a1) the ozone concentration in the supplied air (C_{in}) was set at 0.65 [ppm].   In Case (a2) it was set at 2.44 [ppm]. The effect of the wall surface deposition in the room model were analyzed at each supplied air ozone concentration. The wall surface deposition of ozone was analyzed using Equation (3). For the mass accommodation coefficient, γ, we adopted the value of 8.0×10^{-6} [-] for stainless steel wall surfaces in accordance with Cano-Ruiz et al., 1993.

8 Results of Model Room Experiment

Mean Velocity

We conducted detail measurements of flow fields in the model room by using Laser Doppler Velocimetry (LDV). We confirmed that the two-dimensional flow fields were reproduced in this model room. Details of the modeling experiment were reported in a previous paper. (Kato et al., 2003). In the model room, a large circulating flow was formed along the wall surface in the room, and a secondary vortex opposite the major flow was observed in the floor corner as shown in Figure 4.

Concentration Distributions

The background concentrations of the sum of the chemical compounds (VOC) and Suspended Particulate Matter (SPM) in the supply air were confirmed to be below 30 [μg/m³] and 0.01 [mg/m³] (total concentration of particles of diameter 10μm or less), respectively. Hence, only surface reactions with the stainless steel walls were considered in this model room experiment.

Ozone concentration distributions in the model room for each experiment are shown in Figure 5. The concentration values in the figures are given in [ppm]. In all the experimental cases, ozone should be uniformly distributed in the model room from

Table 2 Numerical conditions

Turbulence Model	Low Re type k-ε model (MKC model, 2-dimensional calc.)
Mesh	220 (x) × 110 (z)
Scheme	Convection Term: QUICK
Inflow Boundary	U_{in} = 3.0 and 2.0 [m/s], k_{in}=3/2× $(U_{in}×0.015)^2$, ε_{in}=C$_\mu$×$k_{in}^{3/2}$/l_{in}, C$_\mu$=0.09, l_{in}=(Slot width) ×1/7
Outflow Boundary	U_{out} = Free slip k_{out}= Free slip, ε$_{out}$ = Free slip
Wall Treatment	Velocity: No slip $k\|_{wall}$: No slip, $\varepsilon\|_{wall} = 2\nu(\partial\sqrt{k}/\partial y)^2$ $\gamma = 8.0\times10^{-6}$, $<v>$ = 360 m/s

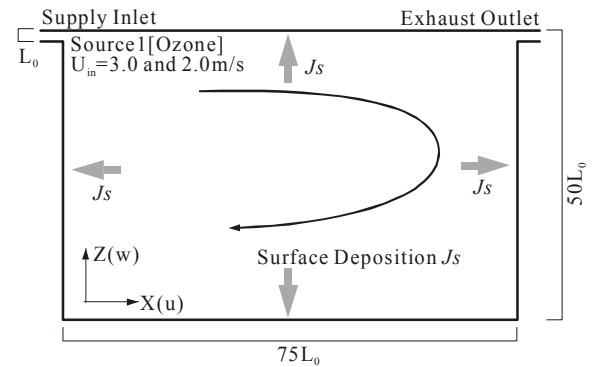Figure 3 Room model analyzed (CFD analysis, 2D)

Table 3 Numerical cases

Exp. Case	C_{in} [Ozone]	[U_{in}]	Js
Case (a1-a)	0.65 ppm	3.0 m/s	Eq. (3)
Case (a1-b)		2.0 m/s	
Case (a2-a)	2.44 ppm	3.0 m/s	
Case (a2-b)		2.0 m/s	

the viewpoint of the law of mass conservation if there is no decomposition in the indoor air and no deposition to wall surfaces.

In Case (e1-a), where ozone is generated in the supply inlet at a concentration of 0.65 [ppm] and U_{in} = 3.0 [m/s], the ozone is not uniformly distributed in the model room as shown in Figure 5 (1). In this case, the concentration of ozone at the center of the cavity has decreased by about 8% compared with its concentration at the supply inlet. In Case (e1-b), the ozone concentration has decreased by about 11% at the center of the cavity. In Case (e1-a) and Case (e1-b), the ratio of the ozone decrease corresponds to the ratio of the supply inlet velocity.

As for other cases, the tendency for the ozone concentration decrease is similar.

9 Results of Numerical Analysis

Mean Velocity

Stream lines predicted by CFD simulation are shown in Figure 6. The numerical results for the low Reynolds number-type k-ε model were consis-

tent with the experimental results, and it was confirmed that they reproduce the flow fields with reasonable accuracy.

Ozone Concentration Distribution with Wall Surface Deposition

The predicted results for the ozone concentration distribution in the model room, taking into account deposition on the stainless steel wall surfaces, are given in Figure 7. The decay in the ozone concentration is caused solely by the effect of wall surface deposition in these cases, and, conceptually, ozone would be uniformly distributed in the model room if there were no wall surface deposition.

As shown in Figure 7, the ozone level decreases along the walls in all cases. The room-averaged concentrations (C_{ave}), the average concentration at exhaust outlet (C_{ext}), and removal of ozone are shown in Table 4.

In the case of U_{in} = 3.0 m/s, the removal ratio of ozone from the room model by ventilation was about 95% and the removal ratio by deposition became about 5%. In the case of U_{in} = 2.0 m/s, the removal ratio of ozone by ventilation was about 92% and the removal ratio by deposition became about 8%. In this analysis, the effect of deposition to the stainless steel wall surfaces was relatively small compared with the removal effect of ventilation. However, deposition to other building materials can be much faster than deposition to stainless steel [Kleno et al., 2001]; such surfaces would be expected to produce larger effects.

Comparisons of the ozone concentration distribution between the CFD analyses and the experiments are shown in Figures 8. The numerical simulations that include wall surface deposition for ozone are reasonably consistent with the experimental results.

10 Mass Balance Model

In order to estimate the validity of the numerical analysis shown in Table 4, an analysis of the mass balance was conducted. In this analysis, we assume the conditions of steady state and perfect mixing in the room model. The mass balance equations are shown in Equations (4) and (5).

$$E_x \cdot C_{o(in)} = E_x \cdot C_{o(out)} + v_d \cdot \left(\frac{A}{V}\right) \cdot C_{o(in)} \quad (4)$$

$$\frac{C_{o(out)}}{C_{o(in)}} = \left(1 - \frac{v_d \cdot \left(A/V\right)}{E_x}\right) \quad (5)$$

Here, E_x [times/sec] is the ventilation rate (in this analysis, E_x = 0.04[times/sec]), v_d [m/s] is the deposition velocity, A [m²] is the surface area of stainless steel, and V [m³] is the chamber volume. In this analysis, we adopt v_d=0.6×10⁻³ in accordance with Nazaroff and Cass (1986). In this case, the predicted ozone decrease ($[C_o]_{out}/[C_o]_{in}$) is 0.95.
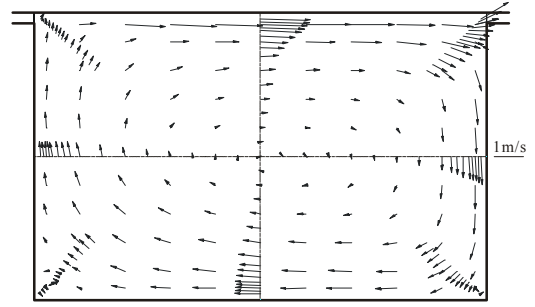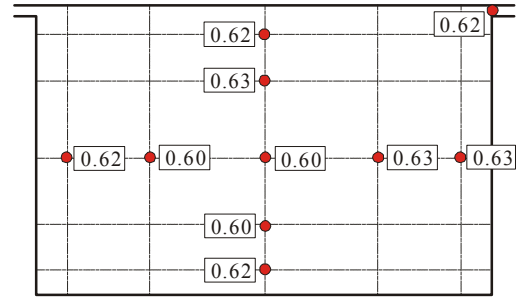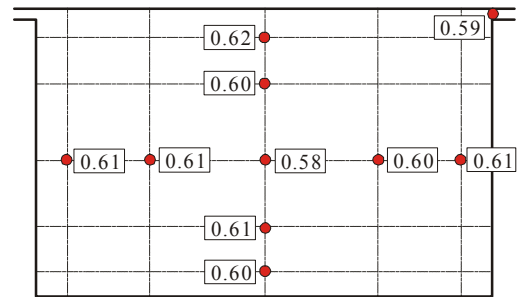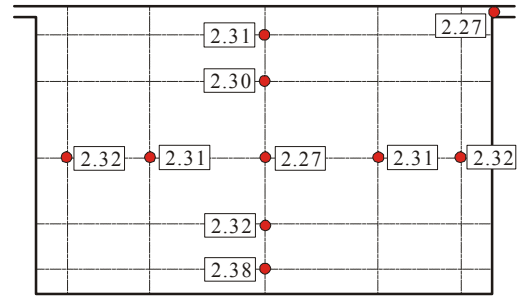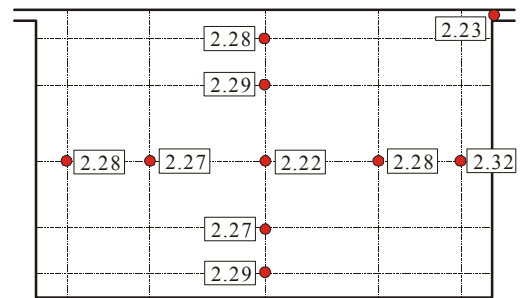

Figure 4 Flow field measured by LDV (U_{in}=3.0 [m/s])

(1) Case (e1-a) (U_{in}=3.0, C_{in}=0.65)

(2) Case (e1-b) (U_{in}=2.0, C_{in}=0.65)

(3) Case (e2-a) (U_{in}=3.0, C_{in}=2.44)

(4) Case (e2-b) (U_{in}=2.0, C_{in}=2.44)

Figure 5 Experimentally determined concentration distributions of ozone (ppm)

The analytical result using the mass balance model is in reasonable agreement with the results from the model room experiment and the numerical analysis based on an ozone deposition flux model.

11 Discussions

In this section, we try to estimate the first-order rate constant k_u [1/sec] and deposition velocity v_d [m/s], from the macroscopic point of view.

If it is assumed that it is possible to model the heterogeneous reaction of ozone with the surfaces by the first-order rate constant k_u [1/sec], the reaction rate of ozone is simply proportional to the elapsed time or staying time (= age of air) in the model room. The age distribution of the supplied air is shown in Figure 9. The age values in Figure 9 were normalized by a nominal time constant τ_n (= V/Q). In this analysis, the age of the air was analyzed using the SVE 3 concept [Kato et al., 1988].

The first-order rate constant k_u can then be estimated using the age distribution shown in Figure 9 and the experimental results shown in Figure 5. The definition of the first order rate constant k_u using the age of the air is given by Equation (6):

$$k_u = \frac{\Delta C_{o(i)}}{C_{o(in)} \cdot t_{a(i)}} \qquad (6)$$

Here, $C_{o(in)}$ [ppm] is the ozone concentration at the supply inlet, $t_{a(i)}$ [sec] is the age of air at position (i), and $\Delta C_{o(i)}$ [ppm] is the decrease in concentration comparing $C_{o(in)}$ with the concentration at position (i).

The resulting first-order rate constants, k_u, which were estimated using Equation (6) are shown in Table 5. The values of k_u in Table 5 are the mean values of ten experimental points (see Figure 2). In Case (e1-a) and Case (e1-b), where the ozone concentration at the supply inlet was 0.65 [ppm], the values of k_u were 9.8×10^{-4} and 9.9×10^{-4} [1/sec] respectively. In Case (e2-a) and Case (e2-b), where the ozone concentration at the supply inlet was 2.44 [ppm], the values of k_u were 8.6×10^{-4} and 8.7×10^{-4} [1/sec] respectively. Hence, for these conditions, k_u remained relatively constant, consistent with expectations. Also, as shown in Table 5, we can estimate the order of the depositon velocity v_d by using estimated k_u and Equation (4). The values of v_d were ranged between 2.6×10^{-4} and 3.0×10^{-4} [m/sec] in this analytical conditions.

12 Concluding Remarks

(1) The concentration distributions of ozone in the model room were measured. The results supported the assumption that the ozone concentration decreased due to deposition on the stainless steel surfaces.
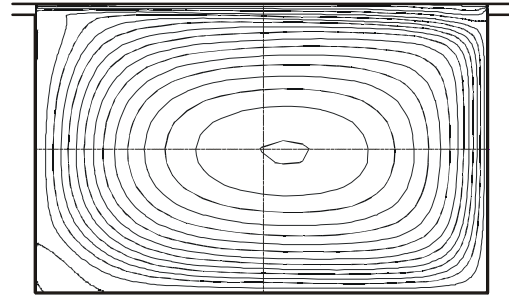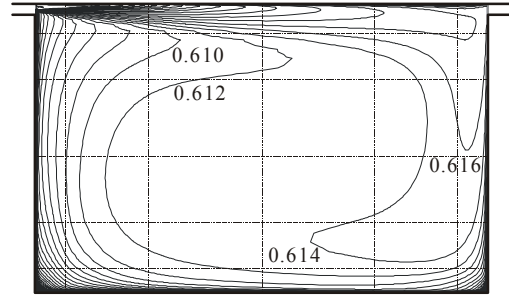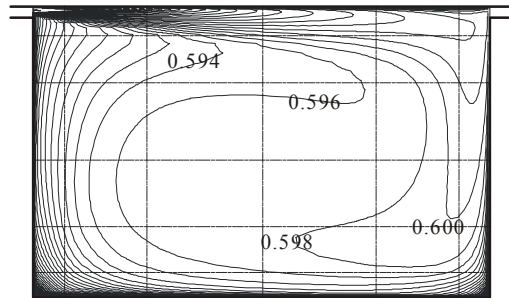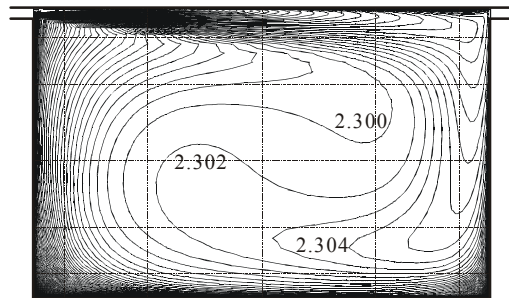
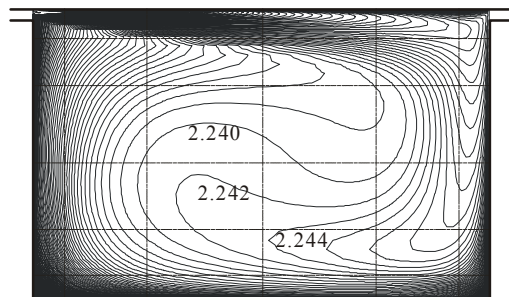

Figure 6 Stream line

(1) Case (a1-a) (U_{in}=3.0, C_{in}=0.65)

(2) Case (a1-b) (U_{in}=2.0, C_{in}=0.65)

(3) Case (a2-a) (U_{in}=3.0, C_{in}=2.44)

(4) Case (a2-b) (U_{in}=2.0, C_{in}=2.44)

Figure 7 Concentration distribution of ozone
(numerical results)

Table 4 Room-averaged concentration
and removal of ozone by CFD

Numerical Case	C_{in} [ppm]	C_{ext} [ppm]	C_{ave} [ppm]	Removal [%]
Case (a1-a)	0.65	0.62	0.61	Ventilation : 94.7 Deposition : 5.3
Case (a1-b)		0.60	0.60	Ventilation : 92.4 Deposition : 7.6
Case (a2-a)	2.44	2.31	2.30	Ventilation : 94.7 Deposition : 5.3
Case (a2-b)		2.25	2.24	Ventilation : 92.4 Deposition : 7.6

(2) The results of numerical prediction and experiment were in good agreement, supporting the validity of the surface deposition flux model for ozone.

(3) The surface removal rate was consistent with reports in the literature for similar surfaces (e.g., see Table 3 in Weschler, 2000).

References

[1] Atkinson R, Hasegawa D, and Aschmann SM (1990). Rate Constants for the Gas-Phase Reactions of O_3 with a Series of Monoterpenes and Related Compounds at 296 K. International Journal of Chemical Kinetics, 22, 871.

[2] Cano-Ruiz JA, Kong D, Balas RB, and Nazaroff WW (1993). Removal of Reactive Gases at Indoor Surfaces: Combining Mass Transport and Surface Kinetics. *Atmospheric Environment* 27A (13), pp. 2039- 2050.

[3] Kato S, Ito K, Murakami S, (2003) Analysis of Visitation Frequency through Particle Tracking Method based on LES and Model Experiment : International Journal of Indoor Air Environment and Health (*Indoor Air*), Volume 13, No.2, pp 182-193

[4] Kato S, Murakami S, (1988) New Ventilation Efficiency Scales Based on Spatial Distribution of Contaminant Concentration Aided by Numerical Simulation. ASHRAE Transactions 94(2), pp. 309- 330.

[5] Kleno JG., Clausen PA, Weschler CJ, and Wolkoff P (2001). Determination of Ozone Removal Rate by Selected Building Products Using the FLEC Emission Cell, Environmental Science & Technology, Vol. 35, No. 12, 2548-2553.

[6] Murakami S, Kato S, and Chikamoto T (1996). New Low Reynolds-number k-ε Model Including Damping Effect Due to Buoyancy in a Stratified Flow Field. *Int. J. Heat Mass Transfer*, 39, 3483- 3496.

[7] Nazaroff WW, Cass GR (1986). Mathematical Modeling of Chemically Reactive Pollutants in Indoor Air, Environ. Sci. Techno. Vol. 20, No. 9, pp. 924-934.

[8] Sørensen DN, and Weschler CJ (2002). Modeling Gas Phase Reactions in Indoor Environments Using Computational Fluid Dynamics. *Atmospheric Environment*, 36(1): 9- 18.

[9] Weschler CJ (2000). Ozone in Indoor Environments: Concentration and Chemistry. Indoor Air 10 (4), pp. 269-288.

[10] Weschler CJ, and Shields HC (2000). The Influence of Ventilation on Reactions Among Indoor Pollutants, Modeling and Experimental Observation. Indoor Air, Vol. 10, No. 2, pp. 92-100.

[11] Weschler CJ, and Shields HC (2003). Experiments Probing the Influence of Air Exchange Rates on Secondary Organic Aerosols Derived from Indoor Chemistry. Atmospheric Environment, Vol. 37: 5621-5631.

[12] Wolkoff P, Clausen PA, Wilkins CK, Hougaard KS, and Nielsen GD (1999). Formation of Strong Airway Irritants in a Model Mixture of (+) –α-pinene/Ozone. Atmospheric Environment, 33, pp. 693-698.

(1) Case (e1-a), (a1-a)

(2) Case (e1-b), (a1-b)

(3) Case (e2-a), (a2-a)
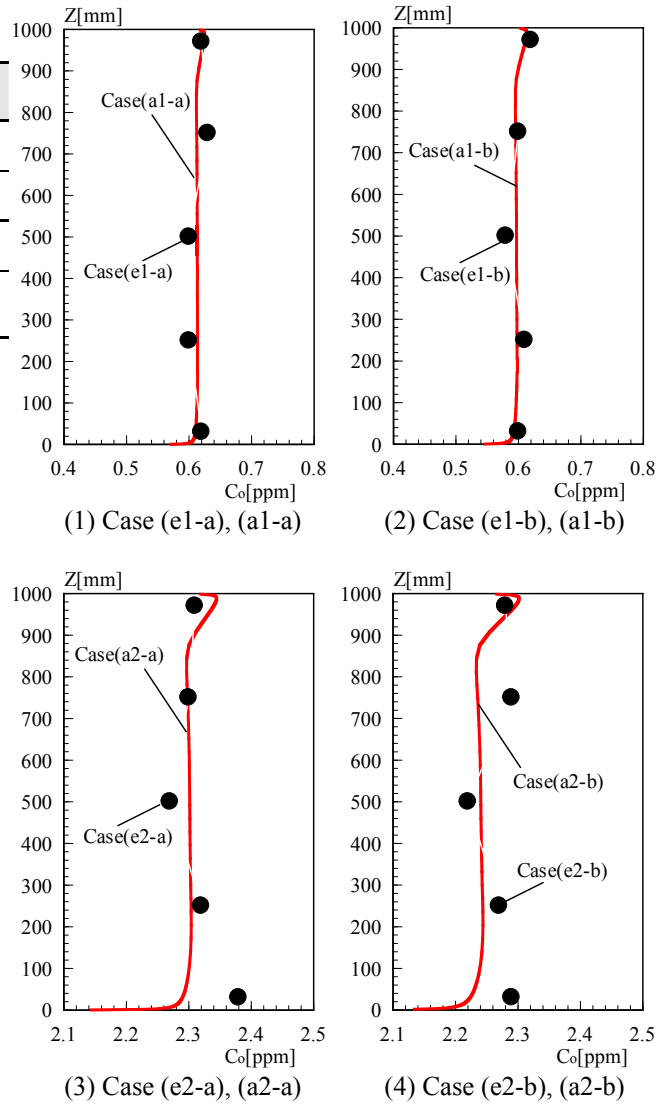

(4) Case (e2-b), (a2-b)

Figure 8 Comparison of ozone concentration
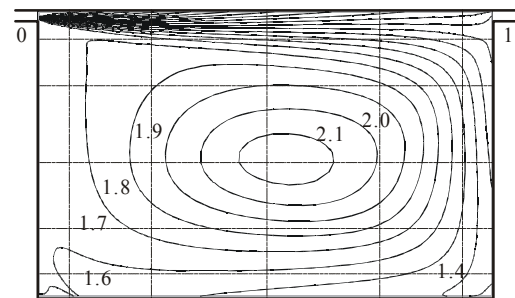(Experiment & prediction, X=750 [mm], Z=0 – 1000 [mm])

Figure 9 Normalized distribution of age of air (SVE 3)

Table 5 Estimated k_u value

Numerical Case	C_{in} [ppm]	U_{in} [m/s]	k_u [1/sec]	v_d [m/sec]
Case (a1-a)	0.65	3.0	9.8×10^{-4}	2.9×10^{-4}
Case (a1-b)		2.0	9.9×10^{-4}	3.0×10^{-4}
Case (a2-a)	2.44	3.0	8.6×10^{-4}	2.6×10^{-4}
Case (a2-b)		2.0	8.7×10^{-4}	2.6×10^{-4}